Epilepsy Research 135 (2017) 1–8

Contents lists available at ScienceDirect

Epilepsy Research

journal homepage: www.elsevier.com/locate/epilepsyres

Microstructural alterations of white matter in juvenile myoclonic epilepsy

Jinnan Gong[a], Xuebin Chang[a], Sisi Jiang[a], Benjamin Klugah-Brown[a], Song Tan[a,b], Dezhong Yao[a,*], Cheng Luo[a,*]

[a] Key Laboratory for NeuroInformation of Ministry of Education, Center for Information in Medicine, High-Field Magnetic Resonance Brain Imaging Key Laboratory of Sichuan Province, School of Life Science and Technology, University of Electronic Science and Technology of China, Chengdu, China
[b] Neurology Department, Sichuan Provincial People's Hospital, The Affiliated Hospital of University of Electronic Science and Technology of China, University of Electronic Science and Technology of China, Chengdu, China

ARTICLE INFO

Keywords:
Juvenile myoclonic epilepsy
White matter microstructure
TBSS
Motor system

ABSTRACT

Juvenile myoclonic epilepsy (JME) is a common type of idiopathic generalized epilepsy that is characterized by myoclonic jerks of the upper limbs and generalized tonic-clonic seizures. Frontal cognitive dysfunctions and abnormal coupling of the thalamocortical system have been found in neuropsychological and neuroimaging studies. This study intended to explore white matter (WM) measurement changes in JME using MRI. Twenty-six patients with JME and 25 healthy controls (HC) were recruited for the acquisition of diffusion MRI and structural MRI data. Then, a tract-based spatial statistics approach was used to investigate the disease effects on WM microstructural diffusion characteristics. Subsequently, the associations between clinical features and characteristics of the tracts that connect the impacted regions were also evaluated. Compared with HC, JME showed an increased mean diffusivity in the anterior corpus callosum connected to the bilateral frontal lobe. Decreased axial diffusivity was observed in the body of the corpus callosum connected to the bilateral supplementary motor area as well as, in the region connecting the left thalamic radiation, the superior longitudinal fasciculus and corticospinal tract. Furthermore, the microstructural metrics of the tracts connecting these regions, especially the projection fibres that connect the cerebral cortex, subcortical regions and cerebellum, were correlated with disease duration. These findings likely reflect the alterations in WM microstructural connectivity, which may be associated with frontal cognitive and motor dysfunction in JME. In addition, the projection fibres connecting these impacted regions are progressively affected by the disease duration. Based on our findings, we propose that the cerebellum may play a potential role in the pathomechanism of JME.

1. Introduction

Juvenile myoclonic epilepsy (JME) is a common idiopathic generalized form of epilepsy, accounting for 5–10% of all epilepsy cases (Janz and Christian, 1957; Panayiotopoulos et al., 1994). Myoclonic jerks and generalized tonic-clonic seizures are the principal characteristics of JME and initially manifest during the mid-teens and mainly occur early in the morning. JME patients reportedly suffer from behavioural disturbances in self-regulation and personality traits, such as impressionability, unreliability, and emotional instability, similar to those of patients with frontal lobe lesions. The pathogenesis of JME has not yet been fully clarified (Hommet et al., 2006). Typical characteristics of electroencephalography (EEG) in JME are 3–4 Hz polyspikes with slow wave discharges and a fronto-central predominance, which are important for clinical diagnosis. Unfortunately, conventional neuroimaging still fails to detect structural abnormalities in JME patients even now.

Nevertheless, increasing neuroimaging evidence supports the theory that JME is involved in abnormalities of the frontal cognitive system, frontal-thalamic network and motor system. A hypothesis that characterized JME by impaired thalamofrontal networks was proposed (Deppe et al., 2008; O'Muircheartaigh et al., 2012) and later reinforced by a MRI spectroscopy study that found decreased thalamic NAA/Cr ratios in patients with JME (Mory et al., 2003). Animal and human studies have suggested that thalamic interactions with the cerebral cortex are involved in the generation of the generalized spike-wave discharges (GSWDs) (Blumenfeld, 2003; Danober et al., 1998; Dong et al., 2016; Li et al., 2016). Moreover, recent studies have demonstrated cognitive dysfunction and abnormal motor function in JME, which could also be induced by an abnormal thalamofrontal network (Bernhardt et al., 2009; Deppe et al., 2008; Jiang et al., 2016).

White matter (WM) alterations in epilepsy patients have been

* Corresponding authors.
E-mail addresses: dyao@uestc.edu.cn (D. Yao), chengluo@uestc.edu.cn (C. Luo).

http://dx.doi.org/10.1016/j.eplepsyres.2017.04.002
Received 17 August 2016; Received in revised form 8 March 2017; Accepted 2 April 2017
Available online 04 April 2017
0920-1211/ © 2017 Elsevier B.V. All rights reserved.

revealed using diffusion magnetic resonance imaging (dMRI) (Luo et al., 2011; Xue et al., 2014; Yang et al., 2012). In patients with JME, Deppe and co-workers studied the fractional anisotropy (FA) of the anterior limb of the bilateral internal capsule, providing structural evidence to support the hypothesis that the thalamocortical network of JME is abnormal (Deppe et al., 2008). Studies merging functional MRI and dMRI found that both functional and structural connections in the prefrontal cortex and motor regions were altered in JME (O'Muircheartaigh et al., 2012; Vollmar et al., 2012). One study revealed that abnormal thalamic connections with the superior frontal and supplementary motor area (SMA) regions may underlie the functional abnormalities in JME. In particular, using the tract-based spatial statistics (TBSS) method, three recent articles that focused on local WM changes in JME have been published. O'Muircheartaigh and colleagues' results revealed decreased FA in two regions of the corpus callosum that connect to the bilateral supplementary motor area and bilateral posterior cingulate cortex, respectively (O'Muircheartaigh et al., 2011). In the findings of Kim and colleagues, differences in WM microstructural metrics were found in the superior corona radiate and forceps minor. These findings likely reflect the structural basis of the frontal lobe dysfunction in patients with JME (Kim et al., 2012). Most recently, a TBSS study demonstrated abnormal WM diffusivity in widespread extra-frontal areas Kim et al., 2015). All of these studies suggest that the WM pathway is affected in JME patients.

Abnormal motor behaviour during seizures is a significant clinical feature of JME patients. Accumulating evidence suggests that altered WM might contribute to this abnormality. However, more evidence is needed to reveal whether the alteration in a key region in the WM affects information transmission between the thalamus and cortex in JME patients. We would like to hypothesize that JME patients may demonstrate significant differences in the motor-related WM pathways and frontal WM, specifically the fronto-thalamic loops, compared with healthy controls (HC). In this study, we acquired high resolution dMRI data and explored WM alterations in patients with JME using TBSS. Subsequently, we investigated the correlations between microstructural measurements and clinical features.

2. Methods

2.1. Participant characteristics

Twenty-six patients with JME (12 males, mean age: 23.5 ± 8.1 years) and twenty-five age-matched healthy controls (12 males, 23.8 ± 5.6 years) were recruited in this study. They were all confirmed as right-handed after performing the Edinburgh Handedness Inventory assessment. JME was diagnosed based on clinical and seizure semiology information consistent with the International League Against Epilepsy (ILAE) guidelines. None of the participants exhibited structural abnormalities detectable by routine MRI, any other seizure types except JME, or any other neurologic or psychiatric disorders. This study was permitted by the ethics committee of the University of Electronic Science and Technology of China (UESTC). After completing a structural clinical evaluation and an assessment of general neuropsychological functions, all subjects were confirmed to exhibit normal cognitive functions. We also assessed the clinical information corresponding to the onset of epilepsy and epilepsy duration (Table 1). MRI data were acquired after the subjects provided their informed consent.

Table 1
Demographic information of subjects.

Label	JME	Healthy controls
General characteristics.		
No.	26	25
Age (years)	23.5 (8.1)	23.8(5.6)
Sex (F:M)	14:12	13:12
Clinical assessment		
Symptom onset (years)	12.8 (6.1)	n/a
Symptom duration (years)	10.7 (7.5)	n/a

2.2. MRI acquisition

MRI data, including diffusion tensor image (DTI) and T1 images, were acquired using a 3.0-T GE Discovery 750 system (GE Medical Systems, Milwaukee, WI) in the Center for Information in Medicine of UESTC. Whole-brain dMRI data were acquired using a single-shot, spin-echo, echo-planar sequence (TR = 8500 ms; TE = 70 ms; voxel size is isotropic 2 mm; FOV = 256 × 256 mm^2; 76 axial slices; 64 diffusion directions; b factor = 1000 s/mm^2). Three sequences without diffusion weighting were also acquired (b = 0 s/mm^2).

Isotropic T1-weighted anatomical images were acquired using a fast-spoiled gradient-recalled echo (FSPGR) sequence (TR = 6000 ms; TE = 2 ms; flip angle = 9°; voxel size 1 × 1 × 1 mm^3).

2.3. MRI preprocessing

Individual T1-weighted anatomical images were nonlinearly registered to a standard T1 image in the Montreal Neurological Institute (MNI) space using the FLIRT tool in FSL (Jenkinson et al., 2012) while preserving the warp image.

Diffusion-weighted images were affine registered to the average of the non-diffusion-weighted volumes to correct for eddy currents and head motion. Non-brain tissues were deleted from the dMRI data using the brain extraction tool (BET) of FSL.

A diffusion-tensor model was applied to the corrected diffusion data at each voxel to acquire the FA and mean diffusivity (MD) map, which was derived from the tensor eigenvalues, including L1, L2 and L3. The L1 is also called the longitudinal diffusivity or the axial diffusivity (AD). The radial diffusivity (RD), which reflects the averaged diffusivities in the two minor axes (L2, L3), was also acquired.

Lastly, all the individual diffusion measurement images were transformed to standard MNI templates by applying the warp image mentioned above after registering individual non-diffusion-weighted images (b0 images) to their own T1 image.

2.4. Statistical analyses

A voxel-wise statistical analysis of the FA map across subjects was performed using tract-based spatial statistics pipelines (Smith et al., 2006). MNI-space FA maps of all subjects were used to generate a mean FA map. Then, the FA maps of all subjects were projected onto a skeletonized FA map derived from the mean FA image, which was thresholded by 0.2. Similar to the FA maps, MNI-space MD, AD, and RD maps were also projected onto the skeleton for further statistical analysis.

Intergroup differences in DTI measurements were analysed using permutation-based non-parametric testing (permuted 2000 times) within the general linear model framework, with age and gender as control variables (Winkler et al., 2014). Finally, threshold-free cluster enhancement (TFCE) was employed (Smith and Nichols, 2009).

2.5. Correlation between WM and clinical indicators

In addition to identifying epilepsy-related WM changes, Pearson's correlation coefficients were calculated between DTI measurements on the skeleton tracts connected to intergroup difference regions that were found in the TBSS analysis and disease duration. False discovery rate (FDR) correction ($P_{FDR} < 0.05$) was performed to adjust for multiple comparisons.

2.6. Presentation

The *tbss_fill script* was applied to all significant maps ($P < 0.05$; TFCE corrected) to enhance visualization. The dilated maps were superimposed on the MNI 152 T1 template brain. Tracts were reported according to the nomenclature of the ICBM-DTI-81 white-matter labels atlas and Johns Hopkins University White-Matter Tractography Atlas.

2.7. Tractography

Probabilistic tractograms, seeding from regions that showed significant intergroup differences in AD and MD, were acquired using FSL's *probtrackx* (probabilistic tracking with crossing fibres) across all participants to further elucidate the anatomic connections of the defined regions from the TBSS analysis. The threshold was set at the value corresponding to the first 1% of the total tracks to binarize the resulting tractograms, which were warped from the native space to the MNI space by applying the warp field generated in the TBSS pipeline. Finally, all tractograms were averaged across subjects and a voxel was preserved only if it been reached in at least 50% of all participants.

3. Results

3.1. TBSS analysis

3.1.1. Differences in MD and AD

Compared with HC, JME patients showed significantly higher MD values ($p < 0.05$ TFCE corrected) in the left forceps minor, a part of the uncinate fasciculus, as well as the joint region connecting the left external capsule, internal capsule and corona radiata (Table 2). Marginally significant increases ($p < 0.005$, uncorrected) in AD and RD in the region showing altered MD in JME were also found (see Fig. S1 in the online version at DOI: http://dx.doi.org/10.1016/j.eplepsyres.2017.04.002). AD reductions in JME patients were observed at the left superior longitudinal fasciculus, left superior corona radiata and left corticospinal tract (CST, including the cerebral peduncle) and a part of the body of the corpus callosum ($p < 0.05$ TFCE corrected, Table 2). Marginally significant decreases ($p < 0.005$, uncorrected) in MD were detected in the above-mentioned regions (see Fig. S1 in the online version at DOI: http://dx.doi.org/10.1016/j.eplepsyres.2017.04.002). This study failed to show a significant difference ($p < 0.05$, TFCE corrected) between JME patients and HC in terms of FA and RD.

Based on the regions with increased MD, schematic tractograms are shown in Fig. 1. One tractogram, seeded from the region showing increased MD in JME patients, traversed the left inferior fronto-occipital fasciculus and uncinate fasciculus. This tractogram demonstrated that the region connects the bilateral frontal pole, superior frontal gyrus and frontal medial cortex. The body of the corpus callosum, which showed decreased AD in JME patients, was found to connect the bilateral supplementary motor area according to its tractogram (Fig. 2). The tractogram seeded from the other cluster with decreased AD in patients, covering primarily the CST that connects the brain stem to the left primary sensorimotor cortex (SM1).

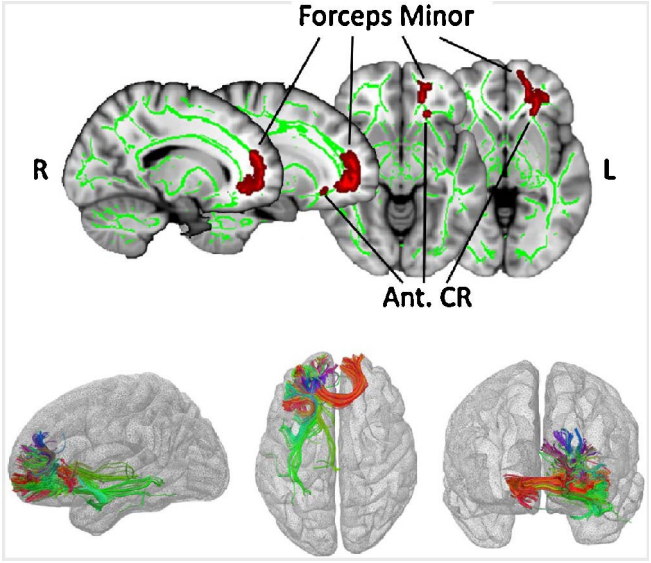

Fig. 1. Group differences in the MD skeleton across the whole brain. The top row demonstrates that JME patients showed significantly higher MD values ($p < 0.05$ TFCE corrected) at the left forceps minor and anterior corona radiata. The bottom row shows the streamline tractogram schematic diagram seeded by the difference region. According to the group results of post hoc probabilistic tracking, this region connects regions, including the bilateral frontal pole, superior frontal gyrus and frontal medial cortex.

3.2. Diffusion measurements in tracts associated with clinical assessments

To investigate disease-related WM changes, the associations between disease duration and diffusion metrics in the tracts with intergroup differences were assessed. Fifteen sections of WM fibres were identified after constraining and segmenting the skeletonized WM using the DTI-81 atlas. These tracts contained the superior cerebellar peduncle, middle cerebellar peduncle, inferior cerebellar peduncle, pontine crossing tract, cerebral peduncle, CST, external capsule, internal capsule, superior longitudinal fasciculus, uncinate fasciculus, superior and anterior corona radiata.

The MD in tracts involving the pontine crossing tract and left inferior cerebellar peduncle were negatively associated with disease duration ($p < 0.05$, FDR corrected, Fig. 3). The MD in tracts, including the middle cerebellar peduncle, left CST and left superior cerebellar peduncle, were also negatively associated with disease duration ($p < 0.05$ uncorrected, Fig. 4). The AD in tracts, including the bilateral cerebral peduncle (left $p < 0.01$, right $p < 0.05$ uncorrected), left CST ($p < 0.05$, FDR corrected, Fig. 3), inferior cerebellar peduncle ($p < 0.01$ uncorrected) and pontine crossing tract ($p < 0.05$, FDR corrected, Fig. 3), were negatively correlated with disease duration. A positive association was found between disease duration and FA in the middle cerebellar peduncle ($p < 0.05$ uncorrected, Fig. 4).

4. Discussion

In the present study, TBSS was used to investigate the differences in the diffusion characteristics between JME patients and HC. MD and AD

Table 2
TBSS results.

Label	Cluster no.	Voxels (> 10)	p value (TFCE corrected)	x	y	z	JHU ICBM-DTI-81 White-Matter Labels	JHU White-Matter Tractography Atlas
Difference in MD. JME > HC	1	742	0.040	−17	43	−7		Forceps minor L,Uncinate fasciculus L
Difference in AD JME < HC	1	412	0.042	−30	−8	14		Superior longitudinal fasciculus L
		104	0.046	−16	−22	−8	Cerebral peduncle L	Corticospinal tract L
	2	269	0.044	−7	−9	27	Body of corpus callosum	

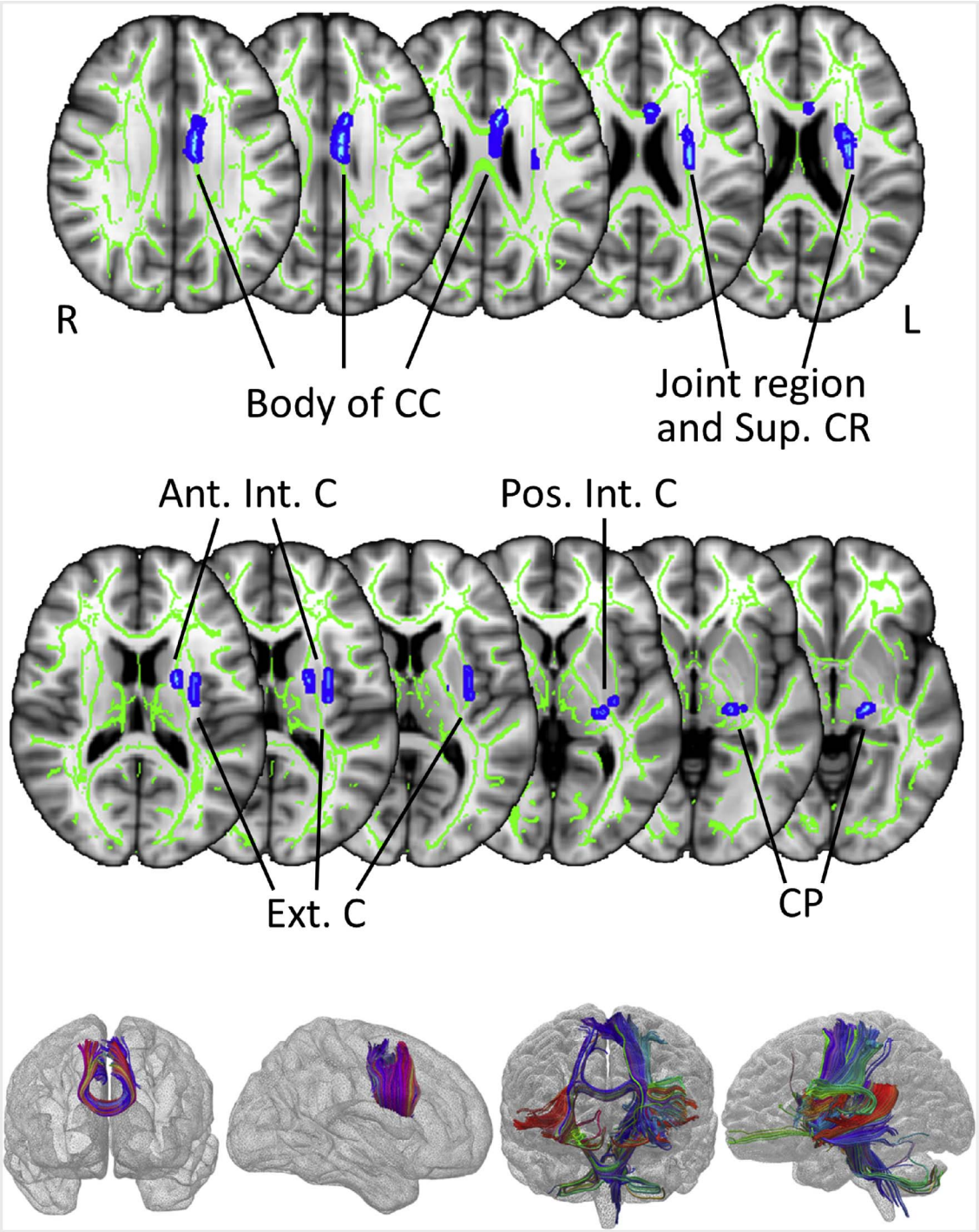

Fig. 2. Group differences in the AD skeleton across the whole brain. The top and middle rows demonstrate that JME patients showed significantly lower AD values in the left superior longitudinal fasciculus, left superior corona radiata, and left CST (including cerebral peduncle) and a part of the body of the corpus callosum ($p < 0.05$ TFCE corrected). The bottom row shows the streamline tractogram schematic diagram seeded by the difference region. According to the group results of post hoc probabilistic tracking, these regions connected the bilateral supplementary motor area and left CST, which connects the brain stem to the left SM1.

in the left forceps minor, corpus callosum and junction region exhibited significant intergroup differences. In general, the alterations in MD and AD may imply the reorganization of the WM microstructure (Dubois et al., 2008). The present results could reflect potential pathological alterations in WM in connection with frontal cognitive and motor functions, which may be associated with frontal cognitive dysfunctions and motor behaviour abnormalities in JME.

The increased MD in the frontal lobe could be associated with damage to the myelin sheath or a reduction of the axon density (Beaulieu, 2002; Song et al., 2002). Studies on JME have indicated impaired frontal lobe functions, including verbal and non-verbal learning (Sonmez et al., 2004) and also verbal and long-term nonverbal memory (Pascalicchio et al., 2007). According to the tractogram seeding from the region that showed intergroup differences in MD, WM impairment in the forceps minor could reflect an abnormal information interaction between the bilateral frontal lobes in JME. This region also contained a part of the uncinate fasciculus, which connects the temporal lobe with the frontal lobe and is associated with linguistic function. Combined with previous studies, alterations in the WM metrics in the forceps minor and uncinate fasciculus may impact

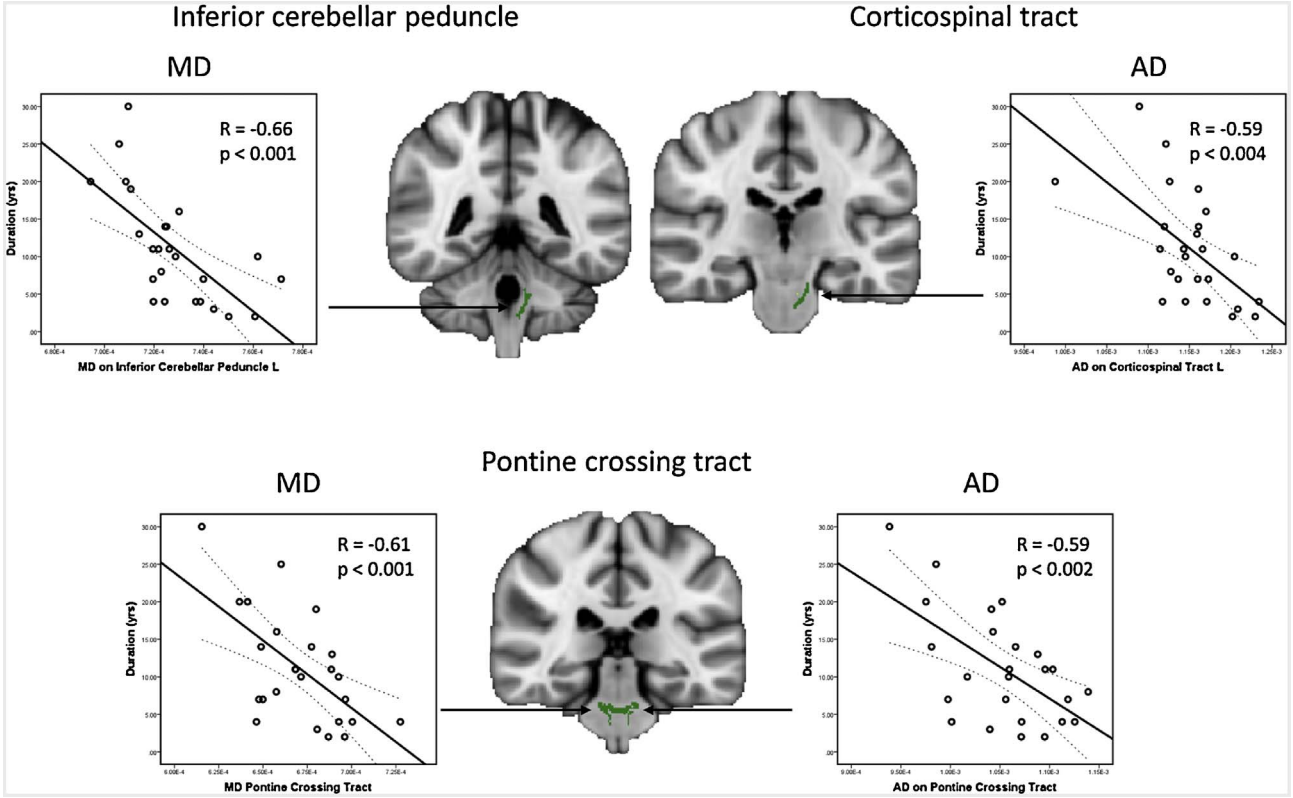

Fig. 3. Significant correlations ($p < 0.05$, FDR corrected) between WM measurements on tracts that connected with intergroup difference regions, which were found in TBSS. The dark green in the figure indicates the location of tracts in which WM measurements were correlated with disease duration. Four negative correlations remained significant, $p < 0.05$, under FDR correction, including correlations between duration of disease with MD of the left inferior cerebellar peduncle (top left), MD and AD of the pontine crossing tract (bottom) and AD of the left CST (top right).

the linguistic-related information interaction between the bilateral frontotemporal lobes.

Another important function of the frontal lobe is working memory. The working memory involves regions including the parietal cortex, cingulate cortex, and parts of the basal ganglia (Diamond, 2013). Impaired working memory function was observed in JME (Swartz et al., 1994). The superior longitudinal fasciculus (subcomponent II, SLF II), which arises from the caudal part of the inferior parietal lobule and terminates in the dorsolateral prefrontal cortex (Brodmann 6, 8 and 46), has been demonstrated to be an important tract for working memory procession. We carefully speculated that the loss of WM integration in the SLF II of JME may reflect the impaired information communication between the frontal and parietal cortices. This obstruction of information could have an effect on working memory. However, because there was no behaviour data for working memory assessed in the present study, more research is warranted in the future to support this assumption.

Damage to thalamocortical circuits in epilepsy patients, especially the fronto-thalamic circuits, was reported in previous studies (Ji et al., 2016; Lin et al., 2009). Here, a reduction in AD and an increased MD was found in the left anterior limb of the internal capsule (covering the anterior thalamic radiation) in JME patients. This finding was consistent with the study by O'Muircheartaigh and co-workers that reported that the abnormal function may be caused by a reduction of structural and functional connectivity in a specific thalamocortical loop (O'Muircheartaigh et al., 2012). A voxel-based morphometry study has revealed that the grey matter volume of the bilateral thalamus was reduced relative to disease progression (Kim et al., 2007). In addition, thalamic and frontal grey matter volumes were associated with executive function in the JME group. EEG and position-emission tomography studies also provided evidence that JME involved fronto-thalamic network dysfunctions (Holmes et al., 2010; Mory et al., 2003). In the present study, the reduced AD and increased MD in the anterior thalamic radiation of JME patients may be interpreted as a loss of WM integration between the frontal lobe and thalamus.

In JME patients, left projection fibres, especially motor-related WM regions, including the anterior and superior corona radiata, internal capsule, external capsule and cerebral peduncle, significantly decreased AD and marginally significantly decreased MD, but no significant alteration in RD or FA was found. Taking these results into consideration, this type of alteration usually implies reorganization of the WM microstructure (Dubois et al., 2008). According to the tractogram, WM reorganization in these regions could impact the connectivity of extensive projection fibres. In detail, the corona radiata, which has been suggested to be impacted in JME according to previous studies (J. H. Kim et al., 2012; S. H. Kim et al., 2015), is a crucial tract that integrates the internal capsule. Reorganization of the corona radiata in JME may influence the motor-related thalamocortical connection as studied by O'Muircheartaigh (O'Muircheartaigh et al., 2012). According to their findings, the alteration of these bundles identified here, which connect the thalamus, prefrontal lobe, premotor cortex and primary motor cortex to transmit motor-related information, may be associated with abnormalities of the motor system of JME patients (Ciumas et al., 2010; Ferlazzo, 2005). Additionally, the cerebral peduncle demonstrated microstructural alterations in this study. The CST conducts impulses from the brain to the spinal cord through the cerebral peduncle. The impaired CST was also found in idiopathic-generalized epilepsy (Focke et al., 2013). We propose a possibility that the alteration, which may result from epileptic activity, would contribute to the motor abnormalities in JME, such as jerks. The cause of this alteration would need further investigation. Moreover, negative correlations between disease duration and diffusion metrics in projection fibres were found. These results further clarified that the WM microstructure in projection fibres, especially the tracts linking to the

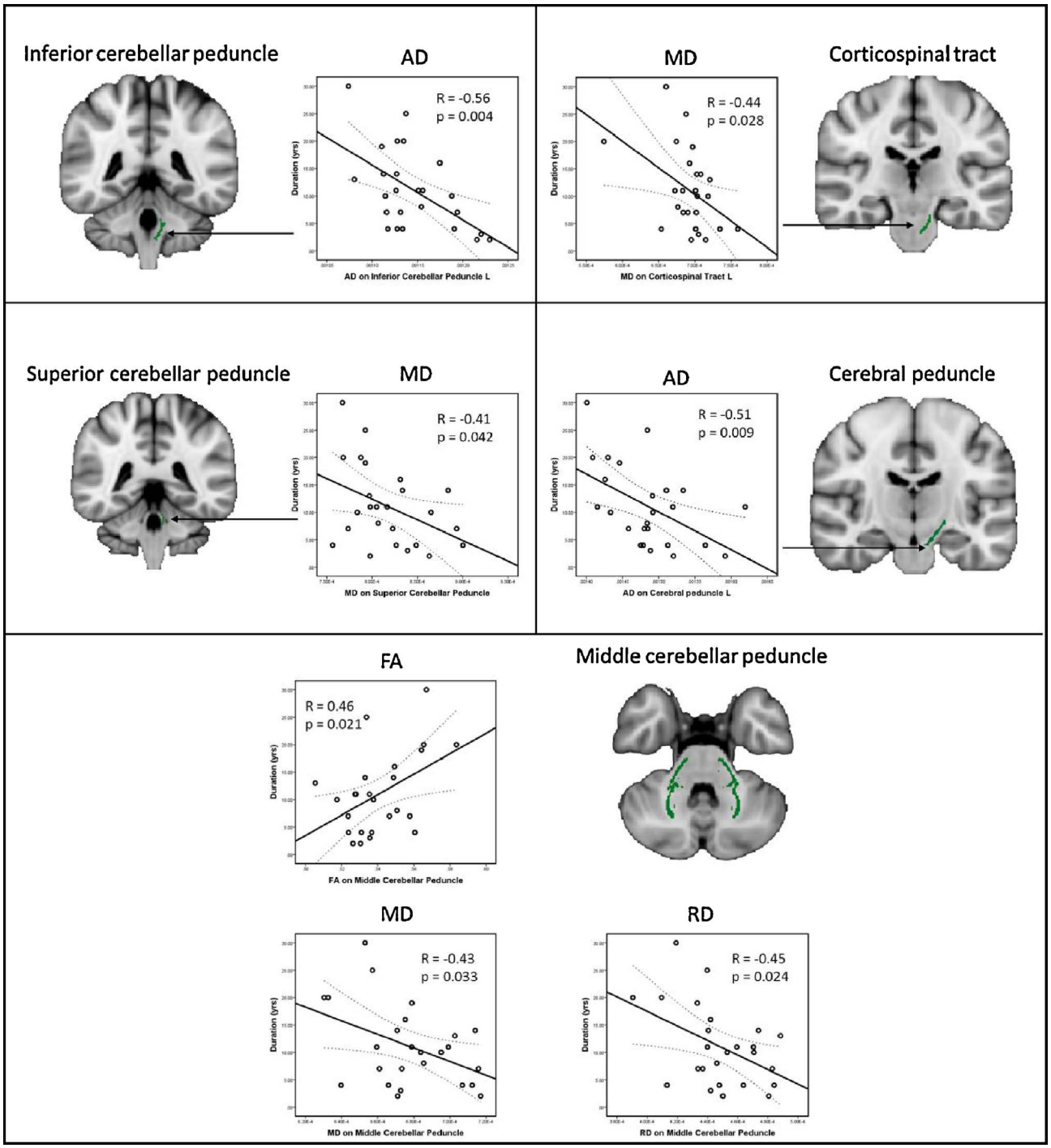

Fig. 4. Marginally significant correlations between WM measurements on tracts connected to the intergroup difference regions, which were found in TBSS. The dark green in the figure indicates the location of the tracts in which WM measurements were correlated with disease duration. AD in the inferior cerebellar peduncle (top left) and in the cerebral peduncle (middle right) and MD in the superior cerebellar peduncle (middle left) and in the CST (top right) were negatively associated with disease duration. FA in the middle cerebellar peduncle was positively correlated to disease duration, but MD and RD in this region were negatively correlated with disease duration (bottom).

cerebral cortex and cerebellum, were gradually reorganized with the progression of disease in JME.

Consistent with previous studies in epilepsy (Luo et al., 2015; Vulliemoz et al., 2010), the reduction in AD in the body of the corpus callosum in JME patients was found to interconnect bilateral SMAs and pre-SMAs based on a checked tractogram. This could reflect the missing link and subsequently reduced interhemispheric inhibition. Additionally, this result may explain the induced hyperexcitability of the bilateral SMA in JME. Furthermore, activation of the SMA and pre-SMA are important for volitional movement or action. The loss of inhibition between the bilateral SMA may be an important pathogeny that could generate myoclonic jerks in JME (O'Muircheartaigh et al., 2012).

A previous study illustrated the widespread and symmetrical disturbances of WM integrity in the frontal lobe and corpus callosum in JME (J. H. Kim et al., 2012). Compared with these findings, this study demonstrated a local impairment in JME, including the joint region of the frontal-related pathways and motor-related pathways. We speculate that the alteration might interrupt the integrity of cognitive and motor-related information.

In addition, we found that the WM microstructure metrics in the cortex-thalamus-cerebellar pathway, such as the cerebellar peduncle and pontine crossing tract, were associated with disease progression. The pontine crossing tract and middle cerebellar peduncle are components of the Cortico-Ponto-Cerebellar pathways (through which they bring information from the cerebral cortex to the cerebellum) (Keser et al., 2015). The superior cerebellar peduncle was a node of the Dentate-Rubro-Thalamo-Cortical pathways (also known as the cerebellar output pathway) (Keser et al., 2015). Although no intergroup differences in cerebellar WM were found directly in the TBSS analysis, these correlations with disease duration may suggest a potential role of the cerebellum in JME.

5. Limitations

The present study illustrated progressive reorganization of the WM microstructure with disease duration. However, to explore the WM alterations with disease progression, further longitudinal designs should be carried out in JME. For example, Yendiki et al. developed a longitudinal diffusion MRI analysis pipeline combination with anatomical priors (Yendiki et al., 2016), which is suitable for detecting subtle longitudinal changes in the WM microstructure of JME due to its high reliability and sensitivity.

In general, JME is a type of idiopathic generalized epilepsy. However, the major intergroup differences in AD and MD were found in three clusters of the left hemisphere. The hemispheric specificity of differences may indicate that WM alterations may be more serious in the dominant hemisphere. This could be researched in the future. The neuropsychological assessments of JME patients were not introduced into the correlation analysis of the present study. Additionally, there is no significant correlation between WM microstructure metrics of the three clusters that showed intergroup differences and disease duration. Therefore, the detailed clinical information would be included in following studies.

The issue of crossing fibre would still be a major problem disturbing findings of dMRI. Partial volume fractions of two fibre orientations were developed to reflect the composition of local fibre bundles. We reconstructed these features at each voxel with the bedpostX tool: f1 and f2, then compared the intergroup difference in f1 and f2 on the skeleton according to the user guide of FSL (Jbabdi et al., 2010). Although no significant intergroup difference in f1 and f2 was found, the effects of crossing fibre on our findings were evident.

6. Conclusion

In summary, altered WM diffusion metrics were observed in two left parts of the corpus callosum, which connects the bilateral frontal cortex and supplementary motor area, and in the joint regions spanning the left thalamic radiation, superior longitudinal fasciculus and CST. It was also found that the WM tracts connected with these regions were progressively reorganized with an increased disease duration. These microstructural alterations may be associated with frontal cognitive and motor dysfunction in JME, providing potential evidence to explain chronic neuropathophysiological abnormalities in patients suffering from JME.

Disclosures

None of the authors has any conflicts of interest to disclose. We confirm that we have read the Journal's position on issues involved in ethical publication and affirm that this report is consistent with those guidelines.

Acknowledgments

This study was funded by grants from the National Nature Science Foundation of China (81271547, 81371636, 81471638), PCSIRT project (IRT0910), and '111' project (B12027).

References

Beaulieu, C., 2002. The basis of anisotropic water diffusion in the nervous system − a technical review. NMR Biomed. 15, 435–455. http://dx.doi.org/10.1002/nbm.782.

Bernhardt, B.C., Rozen, D.A., Worsley, K.J., Evans, A.C., Bernasconi, N., Bernasconi, A., 2009. Thalamo-cortical network pathology in idiopathic generalized epilepsy: insights from MRI-based morphometric correlation analysis. Neuroimage 46, 373–381. http://dx.doi.org/10.1016/j.neuroimage.2009.01.055.

Blumenfeld, H., 2003. From molecules to networks: cortical/subcortical interactions in the pathophysiology of idiopathic generalized epilepsy. Epilepsia 44 (Suppl. 2), 7–15.

Ciumas, C., Wahlin, T.-B.R., Espino, C., Savic, I., 2010. The dopamine system in idiopathic generalized epilepsies: identification of syndrome-related changes. Neuroimage 51, 606–615. http://dx.doi.org/10.1016/j.neuroimage.2010.02.051.

Danober, L., Deransart, C., Depaulis, A., Vergnes, M., Marescaux, C., 1998. Pathophysiological mechanisms of genetic absence epilepsy in the rat. Prog. Neurobiol. 55, 27–57. http://dx.doi.org/10.1016/S0301-0082(97)00091-9.

Deppe, M., Kellinghaus, C., Duning, T., Möddel, G., Mohammadi, S., Deppe, K., Schiffbauer, H., Kugel, H., Keller, S.S., Ringelstein, E.B., Knecht, S., 2008. Nerve fiber impairment of anterior thalamocortical circuitry in juvenile myoclonic epilepsy. Neurology 71, 1981–1985. http://dx.doi.org/10.1212/01.wnl.0000336969.98241.17.

Diamond, A., 2013. Executive functions. Annu. Rev. Psychol. 64, 135–168. http://dx.doi.org/10.1146/annurev-psych-113011-143750.

Dong, L., Luo, C., Zhu, Y., Hou, C., Jiang, S., Wang, P., Biswal, B.B., Yao, D., 2016. Complex discharge-affecting networks in juvenile myoclonic epilepsy: a simultaneous EEG-fMRI study. Hum. Brain Mapp. 37, 3515–3529. http://dx.doi.org/10.1002/hbm.23256.

Dubois, J., Dehaene-Lambertz, G., Perrin, M., Mangin, J.-F., Cointepas, Y., Duchesnay, E., Le Bihan, D., Hertz-Pannier, L., 2008. Asynchrony of the early maturation of white matter bundles in healthy infants: quantitative landmarks revealed noninvasively by diffusion tensor imaging. Hum. Brain Mapp. 29, 14–27. http://dx.doi.org/10.1002/hbm.20363.

Ferlazzo, E., 2005. Cortical triggers in generalized reflex seizures and epilepsies. Brain 128, 700–710. http://dx.doi.org/10.1093/brain/awh446.

Focke, N.K., Diederich, C., Helms, G., Nitsche, M.A., Lerche, H., Paulus, W., 2013. Idiopathic-generalized epilepsy shows profound white matter diffusion-tensor imaging alterations. Hum. Brain Mapp. 35, 3332–3342. http://dx.doi.org/10.1002/hbm.22405.

Holmes, M.D., Quiring, J., Tucker, D.M., 2010. Evidence that juvenile myoclonic epilepsy is a disorder of frontotemporal corticothalamic networks. Neuroimage 49, 80–93. http://dx.doi.org/10.1016/j.neuroimage.2009.08.004.

Hommet, C., Sauerwein, H.C., De Toffol, B., Lassonde, M., 2006. Idiopathic epileptic syndromes and cognition. Neurosci. Biobehav. Rev. 30, 85–96. http://dx.doi.org/10.1016/j.neubiorev.2005.06.004.

Janz, D., Christian, W., 1957. Impulsiv-Petit mal. Deutsche Zeitschrift für Nervenheilkunde 176, 346–386. http://dx.doi.org/10.1007/BF00242439.

Jbabdi, S., Behrens, T.E.J., Smith, S.M., 2010. Crossing fibres in tract-based spatial statistics. Neuroimage 49, 249–256. http://dx.doi.org/10.1016/j.neuroimage.2009.08.039.

Jenkinson, M., Beckmann, C.F., Behrens, T.E.J., Woolrich, M.W., Smith, S.M., 2012. FSL. NeuroImage 62, 782–790. http://dx.doi.org/10.1016/j.neuroimage.2011.09.015.

Ji, G.-J., Yu, Y., Miao, H.-H., Wang, Z.-J., Tang, Y.-L., Liao, W., 2016. Decreased network efficiency in benign epilepsy with centrotemporal spikes. Radiology 160422. http://dx.doi.org/10.1148/radiol.2016160422.

Jiang, S., Luo, C., Liu, Z., Hou, C., Wang, P., Dong, L., Zhong, C., Lai, Y., Xia, Y., Yao, D., 2016. Altered local spontaneous brain activity in juvenile myoclonic epilepsy: a preliminary resting-state fMRI study. Neural Plas. 2016, 1–7. http://dx.doi.org/10.1155/2016/3547203.

Keser, Z., Hasan, K.M., Mwangi, B.I., Kamali, A., Ucisik-Keser, F.E., Riascos, R.F., Yozbatiran, N., Francisco, G.E., Narayana, P.A., 2015. Diffusion tensor imaging of the human cerebellar pathways and their interplay with cerebral macrostructure. Front. Neuroanat. 9, 1–13. http://dx.doi.org/10.3389/fnana.2015.00041.

Kim, J.H., Lee, J.K., Koh, S.-B., Lee, S.-A., Lee, J.-M., Kim, S.I., Kang, J.K., 2007. Regional grey matter abnormalities in juvenile myoclonic epilepsy: a voxel-based morphometry study. Neuroimage 37, 1132–1137. http://dx.doi.org/10.1016/j.neuroimage.2007.06.025.

Kim, J.H., Suh, S.-I., Park, S.-Y., Seo, W.-K., Koh, I., Koh, S.-B., Seol, H.Y., 2012. Microstructural white matter abnormality and frontal cognitive dysfunctions in juvenile myoclonic epilepsy. Epilepsia 53, 1371–1378. http://dx.doi.org/10.1111/j.1528-1167.2012.03544.x.

Kim, S.H., Lim, S.-C., Kim, W., Kwon, O.-H., Jeon, S., Lee, J.-M., Shon, Y.-M., 2015. Extrafrontal structural changes in juvenile myoclonic epilepsy: a topographic analysis of combined structural and microstructural brain imaging. Seizure: Eur. J. Epilepsy 30, 124–131. http://dx.doi.org/10.1016/j.seizure.2015.06.009.

Li, R., Liao, W., Li, Y., Yu, Y., Zhang, Z., Lu, G., Chen, H., 2016. Disrupted structural and functional rich club organization of the brain connectome in patients with generalized tonic-clonic seizure. Hum. Brain Mapp. 37, 4487–4499. http://dx.doi.org/10.1002/hbm.23323.

Lin, K., Carrete Jr., H., Lin, J., Peruchi, M.M., de Araújo Filho, G.M., Guaranha, M.S.B., Guilhoto, L.M.F.F., Sakamoto, A.C., Yacubian, E.M.T., 2009. Magnetic resonance spectroscopy reveals an epileptic network in juvenile myoclonic epilepsy. Epilepsia

50, 1191–1200. http://dx.doi.org/10.1111/j.1528-1167.2008.01948.x.
Luo, C., Xia, Y., Li, Q., Xue, K., Lai, Y., Gong, Q., Zhou, D., Yao, D., 2011. Diffusion and volumetry abnormalities in subcortical nuclei of patients with absence seizures. Epilepsia 52, 1092–1099. http://dx.doi.org/10.1111/j.1528-1167.2011.03045.x.
Luo, C., Zhang, Y., Cao, W., Huang, Y., Yang, F., Wang, J., Tu, S., Wang, X., Yao, D., 2015. Altered structural and functional feature of striato-cortical circuit in benign epilepsy with centrotemporal spikes. Int. J. Neural Syst. 25, 1550027. http://dx.doi.org/10.1142/S0129065715500276.
Mory, S.B., Li, L.M., Guerreiro, C.A.M., Cendes, F., 2003. Thalamic dysfunction in juvenile myoclonic epilepsy: a proton MRS study. Epilepsia 44, 1402–1405.
O'Muircheartaigh, J., Vollmar, C., Barker, G.J., Kumari, V., Symms, M.R., Thompson, P., Duncan, J.S., Koepp, M.J., Richardson, M.P., 2011. Focal structural changes and cognitive dysfunction in juvenile myoclonic epilepsy. Neurology 76, 34–40. http://dx.doi.org/10.1212/WNL.0b013e318203e93d.
O'Muircheartaigh, J., Vollmar, C., Barker, G.J., Kumari, V., Symms, M.R., Thompson, P., Duncan, J.S., Koepp, M.J., Richardson, M.P., 2012. Abnormal thalamocortical structural and functional connectivity in juvenile myoclonic epilepsy. Brain 135, 3635–3644. http://dx.doi.org/10.1093/brain/aws296.
Panayiotopoulos, C.P., Obeid, T., Tahan, A.R., 1994. Juvenile myoclonic epilepsy: a 5-year prospective study. Epilepsia 35, 285–296.
Pascalicchio, T.F., de Araujo Filho, G.M., da Silva Noffs, M.H., Lin, K., Caboclo, L.O.S.F., Vidal-Dourado, M., Ferreira Guilhoto, L.M.F., Yacubian, E.M.T., 2007. Neuropsychological profile of patients with juvenile myoclonic epilepsy: a controlled study of 50 patients. Epilepsy Behav. 10, 263–267. http://dx.doi.org/10.1016/j.yebeh.2006.11.012.
Smith, S.M., Nichols, T.E., 2009. Threshold-free cluster enhancement: addressing problems of smoothing, threshold dependence and localisation in cluster inference. Neuroimage 44, 83–98. http://dx.doi.org/10.1016/j.neuroimage.2008.03.061.
Smith, S.M., Jenkinson, M., Johansen-Berg, H., Rueckert, D., Nichols, T.E., Mackay, C.E., Watkins, K.E., Ciccarelli, O., Cader, M.Z., Matthews, P.M., Behrens, T.E.J., 2006. Tract-based spatial statistics: voxelwise analysis of multi-subject diffusion data. Neuroimage 31, 1487–1505. http://dx.doi.org/10.1016/j.neuroimage.2006.02.024.
Song, S.-K., Sun, S.-W., Ramsbottom, M.J., Chang, C., Russell, J., Cross, A.H., 2002. Dysmyelination revealed through MRI as increased radial (but unchanged axial) diffusion of water. Neuroimage 17, 1429–1436.
Sonmez, F., Atakli, D., Sari, H., Atay, T., Arpaci, B., 2004. Cognitive function in juvenile myoclonic epilepsy. Epilepsy Behav. 5, 329–336. http://dx.doi.org/10.1016/j.yebeh.2004.01.007.
Swartz, B.E., Halgren, E., Simpkins, F., Syndulko, K., 1994. Primary memory in patients with frontal and primary generalized epilepsy. J. Epilepsy 7, 232–241. http://dx.doi.org/10.1016/0896-6974(94)90034-5.
Vollmar, C., O'Muircheartaigh, J., Symms, M.R., Barker, G.J., Thompson, P., Kumari, V., Stretton, J., Duncan, J.S., Richardson, M.P., Koepp, M.J., 2012. Altered microstructural connectivity in juvenile myoclonic epilepsy: the missing link. Neurology 78, 1555–1559. http://dx.doi.org/10.1212/WNL.0b013e3182563b44.
Vulliemoz, S., Vollmar, C., Koepp, M.J., Yogarajah, M., O'Muircheartaigh, J., Carmichael, D.W., Stretton, J., Richardson, M.P., Symms, M.R., Duncan, J.S., 2010. Connectivity of the supplementary motor area in juvenile myoclonic epilepsy and frontal lobe epilepsy. Epilepsia 52, 507–514. http://dx.doi.org/10.1111/j.1528-1167.2010.02770.x.
Winkler, A.M., Ridgway, G.R., Webster, M.A., Smith, S.M., Nichols, T.E., 2014. Permutation inference for the general linear model. Neuroimage 92, 381–397. http://dx.doi.org/10.1016/j.neuroimage.2014.01.060.
Xue, K., Luo, C., Zhang, D., Yang, T., Li, J., Gong, D., Chen, L., Medina, Y.I., Gotman, J., Zhou, D., Yao, D., 2014. Diffusion tensor tractography reveals disrupted structural connectivity in childhood absence epilepsy. Epilepsy Res. 108, 125–138. http://dx.doi.org/10.1016/j.eplepsyres.2013.10.002.
Yang, T., Guo, Z., Luo, C., Li, Q., Yan, B., Liu, L., Gong, Q., Yao, D., Zhou, D., 2012. White matter impairment in the basal ganglia-thalamocortical circuit of drug-naïve childhood absence epilepsy. Epilepsy Res. 99, 267–273. http://dx.doi.org/10.1016/j.eplepsyres.2011.12.006.
Yendiki, A., Reuter, M., Wilkens, P., Rosas, H.D., Fischl, B., 2016. Joint reconstruction of white-matter pathways from longitudinal diffusion MRI data with anatomical priors. Neuroimage 127, 277–286. http://dx.doi.org/10.1016/j.neuroimage.2015.12.003.